Geoinformation Issues
Vol. 6, No 1 (6), 21–35/2013 DOI: https://doi.org/10.34867/gi.2014.2

Integrated Precipitable Water from GNSS as a climate parameter

Michał Kruczyk
Department of Geodesy and Geodetic Astronomy, Warsaw University of Technology,
Pl. Politechniki 1, 00-661, Warsaw, Poland
Tel/Fax: +48 22 2347754, E-mail: kruczyk@gik.pw.edu.pl

Abstract: Tropospheric delay estimates (tropospheric product) on selected International GNSS Service (IGS) and EUREF Permanent Network (EPN) stations exhibit large information potential for meteorology and climate research. Long time series of integrated precipitable water (IPW) averaged hourly, daily and monthly can serve as climate indicators. As IPW is mostly influenced by global circulation, not surface processes, correlations of IPW with basic meteorological surface parameters have been analysed. Even more revealing are changes in correlation coefficients calculated for monthly periods for different regions.
Simple charts of IPW/temperature which can be treated as climatologic diagrams were investigated. Some of these charts have been analysed with some climatologic insight. This form of presenting IPW statistics reveals the variability of seasonal IPW values. IPW clearly represents the diversity of world climates and is a valuable meteorological and climatologic parameter.

Keywords: water vapour, GNSS meteorology, precipitable water vapour, water vapour climatology

Received: 13 March 2015 /Accepted: 28 April 2015

1. Introduction

Atmospheric refraction of the Global Positioning System (GPS) L-band navigational signal manifests itself as tropospheric delay of pseudorange. For a GPS measurement taken for a satellite at zenith and a receiver located at sea level, the Zenith Tropospheric Delay (ZTD), in units of length, amounts to approximately 2.3 m. The ZTDs need to be properly taken into account when high accuracy of determined station coordinates is required, i.e. at the level of several millimetres. Due to the limited accuracy of existing ZTD models, precise applications of GPS positioning (geodynamics, geodetic reference frames), require the estimation of ZTDs in the process of the adjustment of GPS observations, together with other parameters, like station coordinates, phase ambiguities, etc. (Hoffman-Wellenhof et al., 2008; chapter 5.3). Because of temporal variability, ZTDs are usually estimated every hour for each station (24 parameters for a daily session). Tropospheric delay is estimated together with coordinates. The GPS-derived ZTDs obtained from the networks of permanent GPS stations maintained for most precise scientific applications are also used for the purpose of atmospheric research and are the basis of GPS meteorology (Duan et al., 1996). ZTD is a sum of Zenith Wet Delay (ZWD) and Zenith Hydrostatic Delay (ZHD). ZWD, which is about 10% of ZTD depends mostly on the content of water vapour along the path of signal propagation and is highly variable both spatially and temporally. ZHD depends mostly on surface atmospheric pressure, and can be computed at the several millimetre accuracy level from the existing ZHD models using surface meteorological data (Saastamoinen formula with gravitational correction as a function of surface atmospheric pressure is applied).

Integrated Precipitable Water (IPW), sometimes denoted simply as PW, is a valuable meteorological parameter describing quantity of water vapour in the vertical direction over the station in millimetres of liquid water after condensation. A related parameter – Integrated Water Vapour (IWV) – is also used; it has the same value as IPW but is expressed in another unit of measure, i.e. kg/m^2. IPW can be calculated from ZTD by separating Zenith Hydro-

static Delay (ZHD) and Zenith Wet Delay (ZWD) before calculating IPW from previously obtained ZWD with the use of a numerical coefficient dependent on so called "mean temperature" (along the vertical profile of the atmosphere) (Rocken et al., 1993; Bevis et al., 1994). The procedure is presented in detail in the next section.

On the other hand IPW can be determined from vertical humidity data, i.e. radiosounding data or numerical weather prediction models by integrating water vapour density. IPW can also be obtained from the measurements of atmospheric radiation in infrared using radiometers and photometers. A number of studies have shown that IPW estimates from ground-based GPS observations and meteorological/aerological data give the same level of accuracy as aerological techniques. GNSS-derived IPW is the basis of a new discipline called GNSS meteorology, which is developing dynamically (see. e.g. Van der Marel, 2004; Vazquez and Brzezinska, 2012).

2. IGS/EPN tropospheric solutions and IPW determination

Several tropospheric solutions are routinely provided as a result of the IGS and EPN services. These solutions are available in the repositories of Data Centres. The following tropospheric products can be used for research:

- IGS combined product – provided by Gend until the mid-2006;
- new IGS tropospheric product calculated from 2002 by Byun and Bar-Sever, JPL, and from 2011 by Byram, USNO (see Byun and Bar-Sever, 2009);
- EPN (EUREF Permanent Network, http://www.epncb.oma.be) combined product made by Söhne (see Söhne and Weber, 2009) and Pacione (from 2014);
- IGS Analysis Centres' individual solutions: CODE, SIO, NGS, JPL, EMR and EPN Analysis Centres' solutions.

Integrated precipitable water, i.e. total column of water vapour (as liquid) is determined from ZTD solution by a widely known procedure involving first the separation of Wet Delay by calculation of Hydrostatic Delay:

$$\mathrm{ZWD} = \mathrm{ZTD} - \mathrm{ZHD} \tag{1}$$

Physically ZHD is defined as follows:

$$\mathrm{ZHD} = \int_0^{p_s} \frac{R_d k_1}{g}\, dp \tag{2}$$

where p_s is surface atmospheric pressure, R_d is specific gas constant for dry air, g is the acceleration of gravity and non-inertial forces acting upon a particle at rest with respect to the Earth, and empirical constant $k_1 = 7.76 \cdot 10^{-7}$ [K/Pa]. To practically calculate ZHD the Saastamoinen formula has been used:

$$\mathrm{ZHD} = 2.2779\, p / \mathrm{f}(\varphi, H) \tag{3}$$

where p is atmospheric pressure, function f reproduces changes in gravity with latitude φ and ellipsoidal height H in kilometres (Davis et al., 1985):

$$\mathrm{f}(\varphi, H) = (1 - 0.00266 \cos 2\varphi - 0.00028H) \tag{4}$$

In the next step the obtained ZWD is transformed into IPW using the coefficient κ dependent on "mean temperature".

$$\mathrm{IPW} \approx \kappa \cdot \mathrm{ZWD} \tag{5}$$

with κ given as follows:

$$1/\kappa = 10^{-6}\left(C_3/T_m + C_2'\right)R_v \tag{6}$$

where R_v is a specific gas constant for water vapour, T_m is "mean temperature" (through the vertical profile of the atmosphere), C_i are empirical coefficients (given e.g. in Davis et al., 1985). Coefficient κ of a value about 1/6.4 depends on the temperature vertical profile but it can be estimated as a function of surface temperature at the GNSS station (Bevis et al., 1994). For the separation of ZWD direct measurements of meteorological parameters at GNSS stations are needed. Unfortunately the GNSS stations equipped with meteorological sensors are quite sparse.

Both meteorological data which are recorded in different time intervals (from 30 seconds to 30 minutes, depending on the IGS station operator), and ZTD estimates over 5 minute intervals (in the case of the IGS solution) have been averaged in hourly intervals. Only hourly data are the subject of IPW calculation as described above. Figure 1 shows hourly IPW values for JOZE station for the whole of the year 2009.

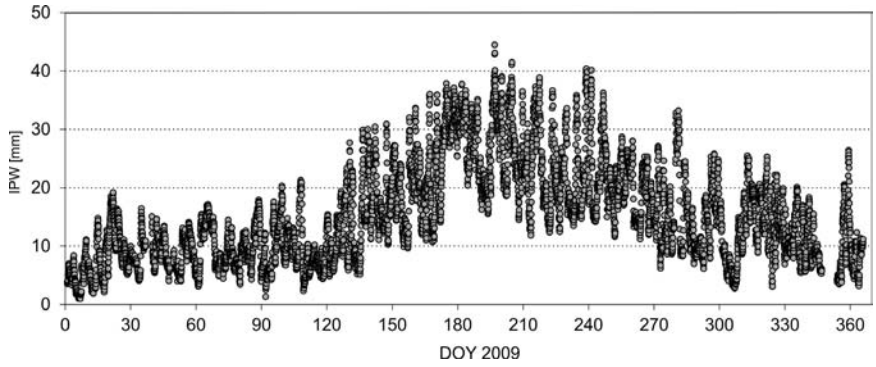

Fig. 1. IPW (from EPN hourly tropospheric combined estimates) for JOZE (Jozefoslaw, Poland) in 2009

First the daily changes in IPW will be analysed. IPW hourly averaged values obtained from IGS data have been averaged over the whole year (in this case 2012). Diurnal IPW variability depends strongly on the season. In winter they are virtually invisible (Fig. 2). However, absolute humidity, i.e. the content of water vapour at the station level, shows a small diurnal cycle (Fig. 3).

Daily IPW changes in the summer season for stations in mid-latitudes (Fig. 4) and in any latitude in the highly oceanic climate (Fig. 5) are unusually small.

Diurnal variations in IPW are a little more pronounced for the summer (IPW maximum in late afternoon). The pattern is shaped not only by atmospheric and ground temperature (radiative ba-

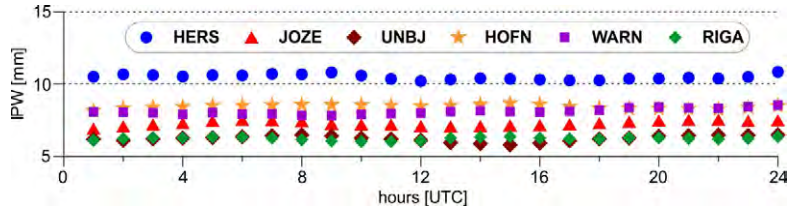

Fig. 2. Hourly averages of IPW in winter (January–February) for HERS (Hailsham, Sussex, UK; almost sea level) and UNBJ (Fredericton, New Brunswick, Canada), HOFN (Hoefn, Iceland), WARN (Rostock-Warnemünde, Germany), JOZE (Jozefoslaw, Poland), and RIGA (Riga, Latvia); IGS tropospheric product, 2009–2013 averages

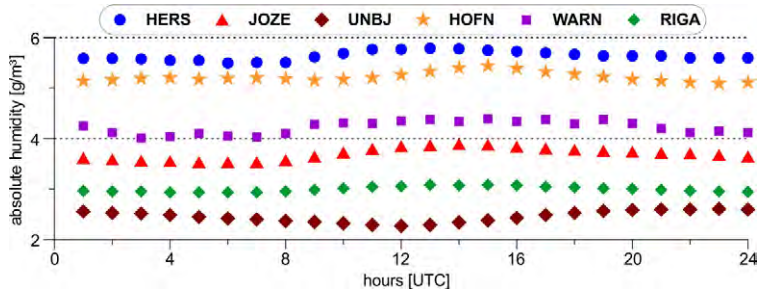

Fig. 3. Hourly averages of absolute humidity in winter (January–February); IGS tropospheric product, 2009–2013 averages

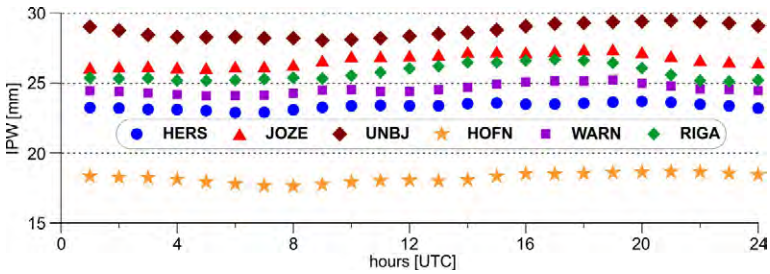

Fig. 4. Hourly averages of IPW in summer (July–August); IGS tropospheric product, 2009–2013 averages

lance) but can also be modified by precipitation (most probable at noon) and local effects (wind patterns, e.g. breeze in the case of WARN, and urban heat island (UHI) in the case of JOZE in the Warsaw agglomeration).

Daily changes in IPW are more visible (clear maximum and minimum) for stations in a continental climate (e.g. ULAB) and points located in a subtropical environment (e.g. DARW). The daily cycle of radiation and humidity at those stations is in its global extreme. This cycle is caused by insolation so its maximum drifts with the station longitude just as local solar midday.

There is only a modest influence of the daily cycle on IPW, which represents the whole of the troposphere, not only the boundary layer, where the

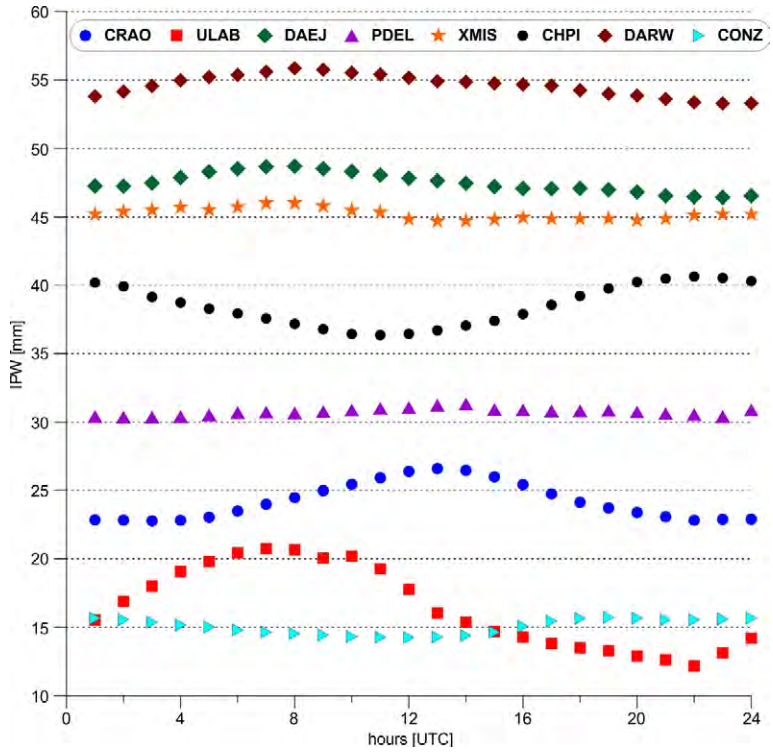

Fig. 5. Hourly averages of IPW in summer (northern hemisphere: July–August; southern hemisphere: January–February) for CRAO (Crimea, Ukraine), ULAB (Ulaanbaatar, Mongolia), DAEJ (Daejeon, South Korea), XMIS (Christmas Island), CHPI (Cachoeira Paulista, Sao Paulo state, Brazil), DARW (Darwin, Australia), PDEL (Ponta Delgada, Azores), and CONZ (Concepcion, Chile); IGS tropospheric product, 2009–2013 averages

evaporation occurs. Relatively small diurnal IPW amplitudes show that IPW is not a local parameter but is affected by advection, shaped over larger areas and in the time scale longer than a day (a water vapour particle lives on average for 9 days from evaporation to condensation).

3. Information on climate in IPW from IGS/EPN tropospheric product

Water vapour is an extremely important (but relatively small) component of the water cycle and plays a crucial role in many meteorological, climatologic and environmental processes (such as evapotranspiration, condensation, precipitation, thermodynamics – latent heat release, cloudiness and its impact on insolation, etc.) as acknowledged in numerous sources (e.g. Shelton, 2009; Andrews, 2010). There are about 15 500 km^3 of water vapour in the atmosphere (only 1/100 000 of all water on Earth). The average value of IPW for the Earth is about 25 mm but average precipitation amounts to about 1000 mm, which exhibits clear evidence of high dynamics of hydrological processes (45 evaporation–condensation cycles in one year). Water vapour contributes to the greenhouse gas effect more than carbon dioxide (but of course lasts in the atmosphere for a short time). In a warmer atmosphere saturation water vapour pressure is higher and water vapour density for the same relative humidity likewise. So water vapour is both climate change agent and indicator. At the same time after condensation in the form of clouds water vapour provides negative radiative forcing. Integrated precipitable water, i.e. column water content in the whole of the atmosphere, provides a convenient measure of water vapour and is obtained by means of GNSS measurements. First it is important to assess the relationship between IPW and surface meteorological parameters. The relationship between integrated precipitable water and temperature is presented in Figure 6.

Figure 7 illustrates the limited content of water vapour in low temperatures. The empirical relationship shown in Figure 7 has a similar form to saturated water vapour pressure (or density) as a function of temperature (compare McIlven, 2010, Fig. 6.2). Humidity in the polar oceanic climate is mostly high – close to saturation. Figure 8 shows the rather complicated relation IPW – atmospheric pressure at the GPS antenna level. Atmospheric pressure for ISTA (elevation of 110 m) is always higher than for CHPI at the elevation of 630 m. The weak correlation of IPW and absolute humidity (Fig. 9) illustrates the deficiency of surface humidity data for modelling IPW with the use of surface meteorological data. Details for more stations of different climates are presented in Table 1.

Some features of correlation coefficient distribution, e.g. some dependencies on GNSS station latitude, can be discerned. Such an effect simply testifies that seasonal differences diminish with latitude so the annual correlations are weaker (Fig. 10).

More interesting still are different patterns of correlation coefficient distribution for the subsequent months (to improve the reliability a multi-

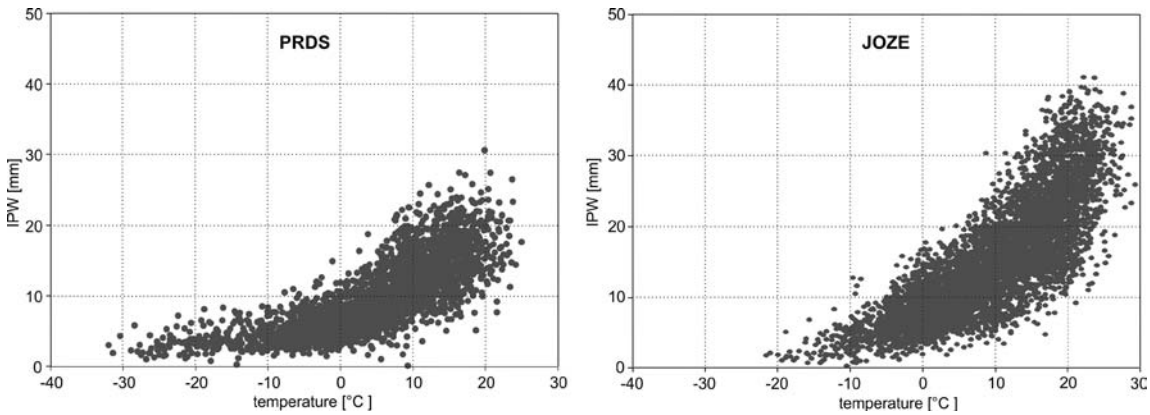

Fig. 6. IPW vs. surface temperature (daily averages) for PRDS (Calgary, Canada) and JOZE (Jozefoslaw, Poland); multi-year series, ZTD from IGS tropospheric product

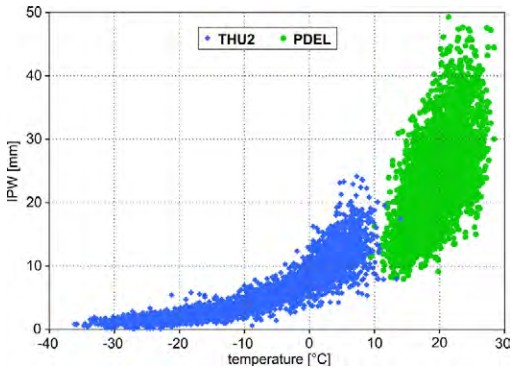

Fig. 7. Integrated precipitable water vs. atmospheric temperature for THU2 (Thule, Greenland) and PDEL (Ponta Delgada, Azores)

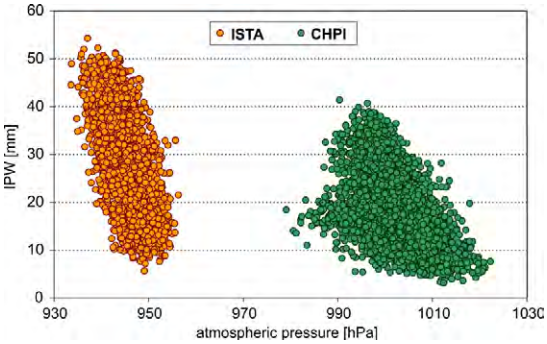

Fig. 8. Integrated precipitable water vs. atmospheric pressure for ISTA (Istanbul, Turkey) and CHPI (Cachoeira Paulista, Sao Paulo state, Brazil)

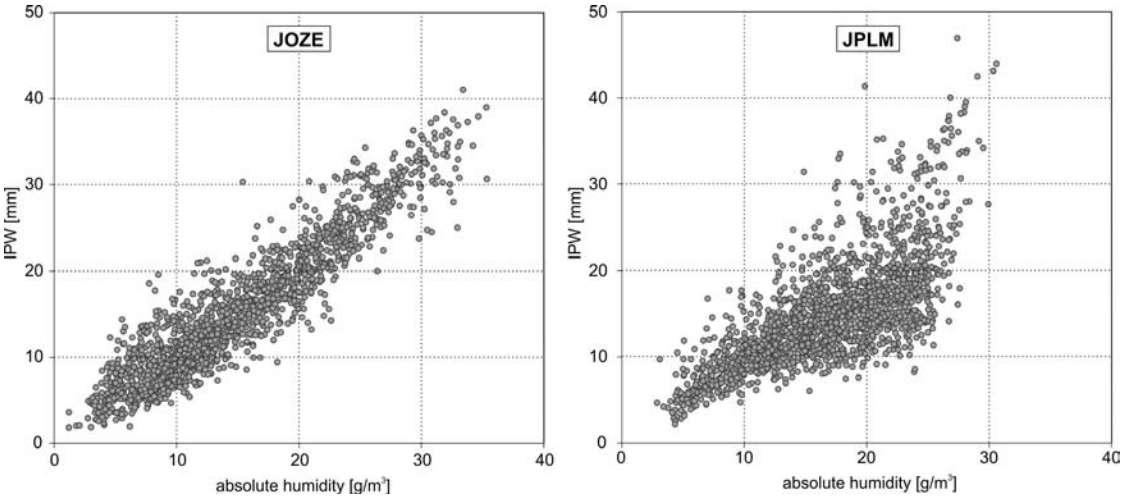

Fig. 9. Integrated precipitable water vs. local absolute humidity [g/m^3] for JOZE (Jozefoslaw, Poland) and JPLM (Pasadena, California, USA)

year series has been used). Changes of seasons are clearly reflected in the correlation coefficient value (Fig. 11). Seasonal influence is different in different locations (most dry air masses in the summer come in the form of a continental hot low, but cold high in the winter). Also different patterns of air mass circulation are possible, e.g. humidity in California (CLAR) is determined by a cold ocean (Californian Current and wet Pacific High). Local weather patterns like geostrophic wind direction and active month differently. atmospheric air masses affect the weather in a given

For the relatively close locations of Warsaw (JOZE) and Berlin (POTS) remarkably similar patterns were obtained (Fig. 12). In some cases there is no IPW – pressure anti-correlation: REYK (Reykjavik, Iceland) is strongly influenced by a permanent global weather feature – Icelandic High – while QAQ1 (Qaqortoq, Greenland) lies at the edge of a massive glacier so a high pressure area is always at the side of the land (Fig. 13).

A stronger anti-correlation in the winter for stations in Europe (at the borders of the vast Asian continent) is natural because high pressure comes as a cold, dry continental air mass (Fig. 14). In the summer the situation is more complicated: high pressure can come both from the north (as dry and cold) but also from the Atlantic (Azores High) as wet and relatively warm air (Fig. 12).

Table 1. Correlation coefficients: IPW – atmospheric pressure (p), IPW – absolute humidity (e), IPW – temperature (T), for selected IGS stations

Station	Years	No. points	Latitude	ASL height	IPW – p	IPW – e	IPW – T
JOZE	1997–2013	5721	52.086	109.3	–0.208	0.751	0.818
LAMA	2001–2013	3682	53.892	157.7	–0.280	0.385	0.629
WROC	2002–2013	3187	51.113	140.7	–0.244	0.675	0.821
GOPE	2002–2013	3721	49.914	546.8	–0.158	0.713	0.762
ZIMM	1997–2013	5614	46.877	907.2	0.016	0.712	0.823
WTZR	1997–2013	4739	49.144	619.1	–0.062	0.779	0.812
POTS	1997–2011	4360	52.380	133.7	–0.220	0.733	0.812
PTBB	2002–2013	4003	52.296	86.9	–0.252	0.903	0.816
HERS	1999–2013	4708	50.867	31.0	–0.165	0.642	0.813
MATE	1999–2013	4476	40.649	489.4	–0.852	0.129	0.290
ISTA	2003–2013	3305	41.104	109.8	–0.482	0.720	0.774
ANKR	2002–2013	3218	39.888	937.1	–0.481	0.597	0.773
PDEL	2002–2013	4073	37.748	54.0	–0.122	0.339	0.327
REYK	2001–2013	4110	64.139	26.6	0.068	0.584	0.805
HOFN	2002–2013	3526	64.267	17.3	0.056	0.690	0.819
QAQ1	2003–2013	3710	60.715	72.8	0.273	0.753	0.779
THU2	2003–2013	3796	76.537	19.3	0.031	0.875	0.869
THU3	2003–2013	3888	76.537	19.3	0.032	0.871	0.866
YSSK	2000–2013	3966	47.030	65.8	–0.206	0.798	0.839
KIT3	2004–2013	2712	39.140	679.7	–0.847	0.330	0.101
WUHN	2002–2013	2748	30.532	39.4	–0.767	0.466	0.760
LHAS	1997–2013	4011	29.657	3656.7	–0.121	0.750	0.748
CHUR	2000–2010	3159	58.759	30.3	–0.541	0.782	0.783
STJO	2000–2009	2857	47.595	142.2	0.059	0.736	0.782
NRC1	2000–2013	3454	45.454	115.5	–0.287	0.720	0.731
PRDS	2000–2009	2865	50.871	1262.7	0.170	0.810	0.759
JPLM	2000–2012	4158	34.205	457.8	–0.375	0.539	0.357
HOLP	2002–2011	3146	33.920	29.2	–0.464	0.753	0.495
CLAR	2002–2011	2969	34.110	406.0	–0.415	0.450	0.524
USNO	1997–2008	3466	38.919	81.1	–0.284	0.789	0.744
CHPI	2003–2013	2781	–22.687	629.9	–0.634	0.588	0.529
THTI	2001–2013	4090	–17.577	91.7	–0.024	0.133	0.384
OHI2	2002–2013	3440	-63.321	18.3	–0.386	0.488	0.061

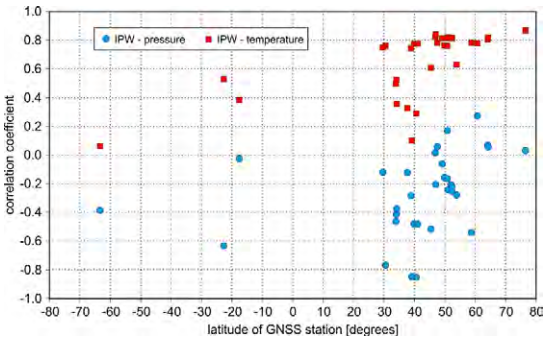

Fig. 10. Correlation coefficients IPW-temperature and IPW-atmospheric pressure as a function of station latitude (33 stations listed in Table 1)

In California (CLAR in Fig. 9) in the winter there are conflicting high pressure areas: continental (Canadian High) and Pacific High, so there is a weak pressure – IPW anti-correlation, and no temperature – IPW correlation. During the Californian summer a positive IPW – pressure correlation can be observed. There are two dominant air masses: Pacific High – cold but wet; continental thermal low – hot but extremely dry (Fig. 15).

Dominant air masses in the various regions for winter and summer are presented in Ahrens (2011, Chapter 10, Fig. 10.3) and Salby (2012, Chapter 15, Fig. 15.9).

Seasonal changes in atmospheric circulation and dynamics can be assessed to some degree also from ZTDs themselves. Monthly correlations of EPN tropospheric delay product for close and more distant station pairs (matched for every station) show a quite different pace of decorrelation with distance for February and July 2009 (Fig. 16).

Daily averaged IPW values obviously carry some climatological information. Figure 17 illustrates the IPW series for GPS stations in drastically different climates (polar and subtropical), i.e. THU2 – north of Greenland; and PDEL – Azores.

A climate diagram similar to the Walter diagram used in climatology can be created (original Walter diagram sets monthly averages of temperature and precipitation) using monthly averages of IPW from multi-year time series. Selected such diagrams are presented in Figure 18.

Figure 18 includes only stations from the Northern Hemisphere so Figure 19 presents two stations from the southern hemisphere, both from the tropical zone. Figure 20 sets together two polar stations, one from the Arctic and the second from the Antarctic Peninsula.

This type of climatologic chart provides even some details which allow the local climate to be described. Figure 21 shows an IPW modified climatologic diagram of temperature and IPW differ-

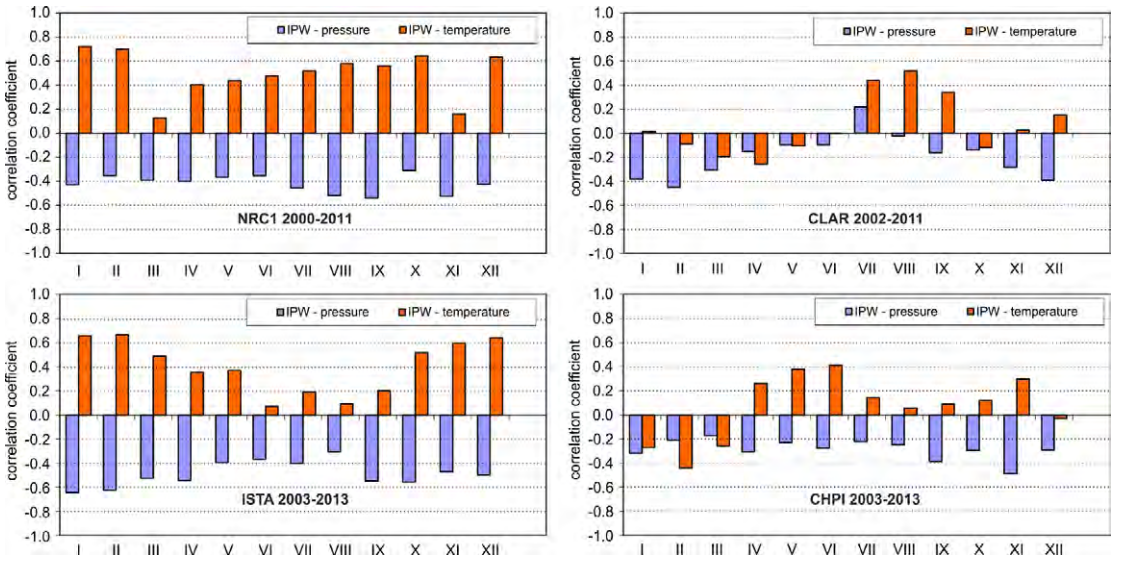

Fig. 11. Monthly correlation coefficients (IPW-temperature and IPW-atmospheric pressure) for NRC1 (Ottawa, Canada), CLAR (Claremont, California, USA), ISTA (Istanbul, Turkey) and CHPI (Cachoeira Paulista, Sao Paulo State, Brazil); multi-year series

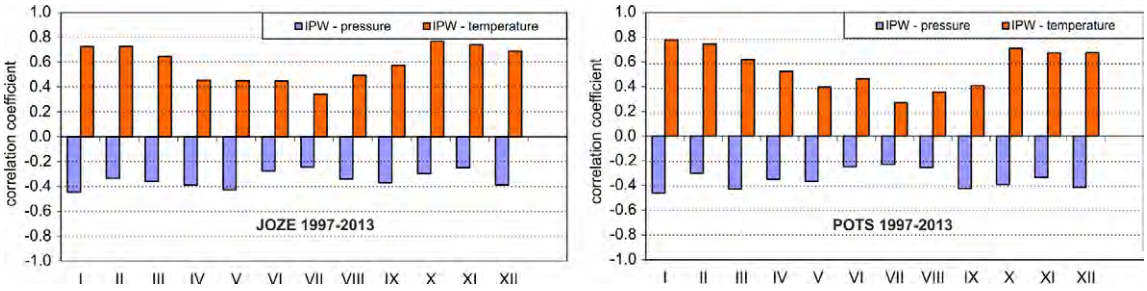

Fig. 12. Monthly correlation coefficients (IPW-temperature and IPW-atmospheric pressure) for JOZE (Jozefoslaw, Poland) and POTS (Potsdam, Germany); multi-year series

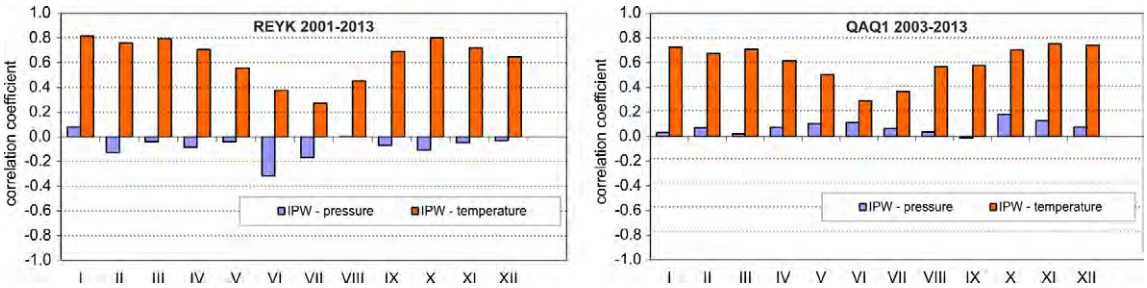

Fig. 13. Monthly correlation coefficients (IPW-temperature and IPW-atmospheric pressure) for REYK (Reykjavik, Iceland) and QAQ1 (Qaqortoq, Greenland); multi-year series

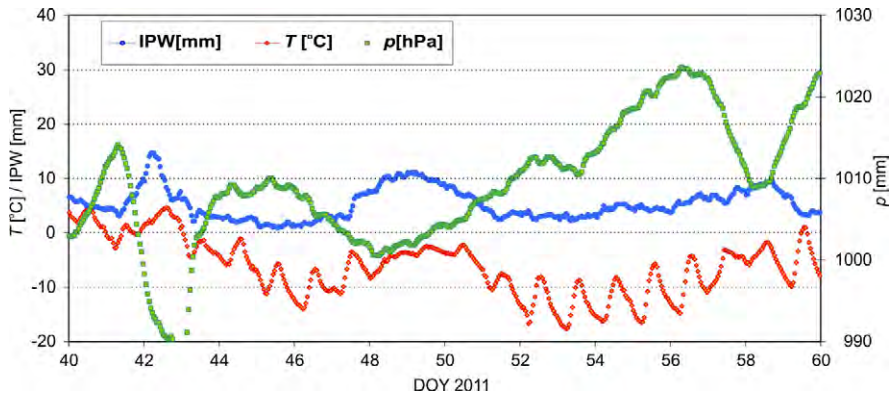

Fig. 14. IPW, atmospheric pressure and temperature at JOZE (Jozefoslaw, Poland), end of February 2011, IGS tropospheric solution

ences for two stations located in Poland: WROC (Wroclaw) is slightly warmer than JOZE except for February (JOZE is closer to the sea).

An especially interesting case is the comparison of ISTA (Istanbul) and ANKR (Ankara) – both stations are in Turkey but Istanbul has a Mediterranean climate whereas that of Ankara, lying in the middle of Anatolia (surrounded by mountains), is more continental and dry (Fig. 22).

Some climate characteristics by means of IPW monthly values can be emphasized simply by setting the monthly values together. Figure 23 shows IPW monthly (multi-year) averages for three stations with a different distance from the ocean.

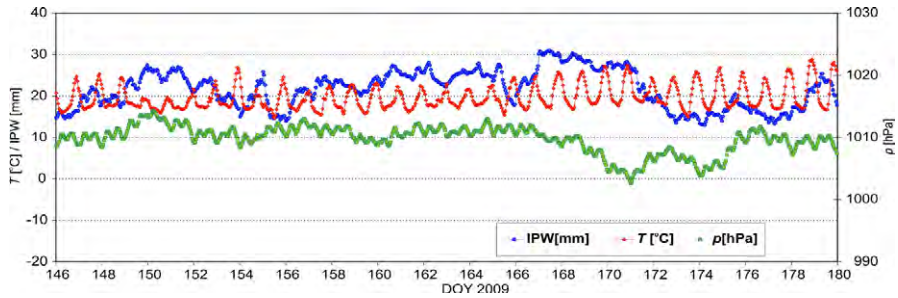

Fig. 15. IPW, atmospheric pressure, and temperature at HOLP (Hollydale, California, USA) end of May-June 2009, IGS tropospheric solution; note wet high DOY 150 and dry low after DOY 171

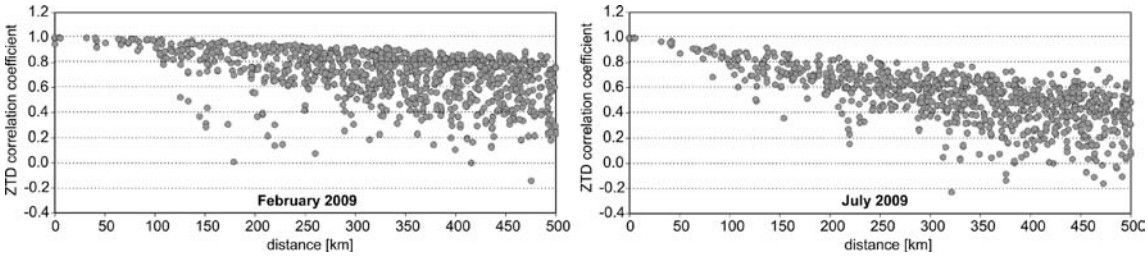

Fig. 16. ZTD correlations for EPN GNSS station pairs in February 2009 and in July 2009

Even some local climate characteristics can be discernible. IPW from IGS tropospheric products can be treated also as an information source for aerology: it demonstrates some clear physical effects evoked by station location (e.g. height, distance from the ocean) and weather patterns like dominant wind directions. Comparison of IPW monthly averages for three GNSS stations in the Los Angeles area, California, USA (Fig. 24) gives some clues to local climate: HOLP (Hollydale) lies closer to the ocean, JPLM (Pasadena) in the hills (450 m ASL) and CLAR (Claremont) also quite high (450 m ASL) but to the east, deeper inland. The map in Figure 25 shows station location in the continent landmass.

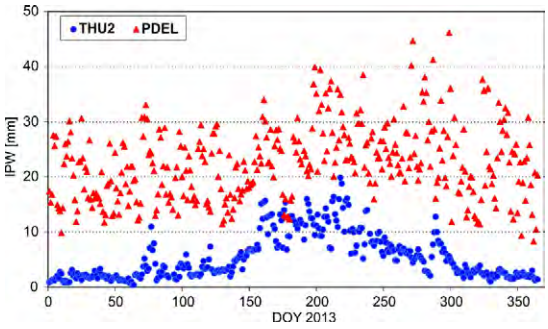

Fig. 17. Daily mean IPW in 2013 for THU2 (Thule, Greenland) and PDEL (Ponta Delgada, Azores); IGS tropospheric product

Monthly IPW averages for the stations investigated are presented in Table 2. Characteristic regularities in the data for the stations not presented before are as follows:

- MATE (Matera) is in the Mediterranean, where winter is more 'humid' than for the Czech Republic (GOPE) or Germany (WTZR, POTS, PTBB), but summer IPW for Matera do not exceed IPW for PTBB (Braunschweig) because of arid air masses in Italy;
- PTBB is closest to the North Sea of German stations listed and is the most 'humid', whereas WTZR has the greatest altitude;
- HOFN and REYK are both located in Iceland;
- QAQ1 (Greenland) has a relatively late maximum in August (the Arctic warms slowly);

Table 2. IPW monthly averages for IGS stations investigated (ZTD from IGS tropospheric delay product); multi-year averages in the periods listed in Table 1

Station	Jan	Feb	Mar	Apr	May	Jun	Jul	Aug	Sep	Oct	Nov	Dec
REYK	8.8	8.4	8.7	10.2	11.7	15.7	18.7	18.2	15.8	12.3	10.2	9.8
HOFN	8.4	8.4	8.9	10.0	11.0	15.0	18.5	18.1	15.6	11.7	10.1	8.3
HERS	11.5	11.0	11.9	13.5	17.0	21.3	23.7	24.1	21.4	19.0	14.5	11.9
LAMA	8.1	7.7	8.3	11.3	16.9	20.3	25.5	24.0	18.6	14.0	11.7	11.4
JOZE	8.1	8.1	8.4	11.7	16.8	21.9	26.1	24.3	18.4	14.7	12.3	9.1
WROC	8.2	7.9	9.1	12.1	17.1	22.2	26.2	25.3	19.3	15.3	12.9	9.3
GOPE	8.3	8.3	8.9	11.5	16.6	20.4	22.8	22.5	17.5	14.3	12.0	9.3
WTZR	7.1	7.0	8.2	10.4	15.0	19.6	21.6	21.6	16.3	13.1	10.3	7.9
PTBB	10.4	9.4	10.6	13.4	18.8	22.8	26.7	26.5	21.7	17.7	14.2	10.9
POTS	8.2	8.1	9.3	11.6	16.7	20.4	24.5	24.1	19.0	14.7	12.4	9.0
ZIMM	7.2	7.1	8.8	11.2	15.3	19.0	21.0	21.1	17.6	14.3	10.2	8.0
MATE	11.2	16.0	11.2	13.5	17.0	21.2	23.1	24.6	22.6	19.1	14.4	11.5
ISTA	11.7	11.8	12.6	15.5	19.8	24.3	26.9	26.4	24.2	20.8	15.8	13.5
ANKR	8.2	8.0	8.5	11.5	15.1	18.0	20.2	19.0	16.4	14.3	10.6	8.9
PDEL	18.9	17.5	18.0	19.8	20.9	25.9	28.1	31.2	28.8	26.2	20.5	19.8
THU2	1.8	2.0	2.1	3.0	5.8	10.3	12.8	12.1	7.5	5.4	3.3	2.6
QAQ1	5.6	5.5	5.6	7.6	9.7	13.9	16.6	16.8	12.2	8.8	7.5	5.6
CHUR	3.3	2.9	4.6	6.4	9.6	14.2	20.4	20.4	14.0	9.5	5.9	3.7
STJO	7.7	7.7	8.6	11.3	14.4	19.3	26.4	24.9	20.1	15.7	12.7	9.7
NRC1	6.0	5.9	9.1	11.3	17.1	24.5	27.3	26.0	21.3	15.0	12.7	7.4
PRDS	5.1	5.1	6.1	7.7	10.6	14.5	17.3	15.9	12.4	8.8	6.3	5.2
DRAO	8.5	7.2	8.0	9.3	13.0	15.8	18.4	18.1	15.1	12.1	9.9	8.1
USNO	12.0	10.7	12.8	17.5	23.6	32.0	37.5	36.3	28.4	20.3	15.2	11.5
CLAR	9.8	10.4	10.9	12.1	14.6	16.4	23.3	21.0	16.7	14.7	11.3	10.2
JPLM	10.3	10.9	11.3	12.3	14.5	15.8	21.8	20.4	17.1	15.2	11.8	10.7
HOLP	11.9	12.6	12.7	14.1	16.6	18.8	25.8	22.6	19.5	17.2	13.5	12.7
WUHN	13.7	17.5	20.1	26.9	35.5	47.3	58.2	55.1	44.4	28.2	19.7	12.9
YSSK	3.7	3.8	5.4	8.8	14.4	22.4	30.8	30.6	20.8	12.0	7.3	4.7
LHAS	5.0	5.8	7.2	9.8	13.7	19.6	24.2	23.2	18.7	11.3	6.3	5.3
KIT3	17.1	17.5	17.1	17.8	21.3	21.1	20.2	19.3	16.6	16.3	14.6	15.9
CHPI	39.9	37.4	36.6	31.8	23.3	19.8	19.4	19.2	23.6	31.3	34.0	38.1
THTI	45.5	45.9	43.7	42.8	38.3	34.5	31.3	31.1	33.5	36.8	42.0	45.1
OHI2	8.5	8.4	8.1	6.7	6.0	4.3	4.3	3.9	5.1	6.1	6.7	7.7

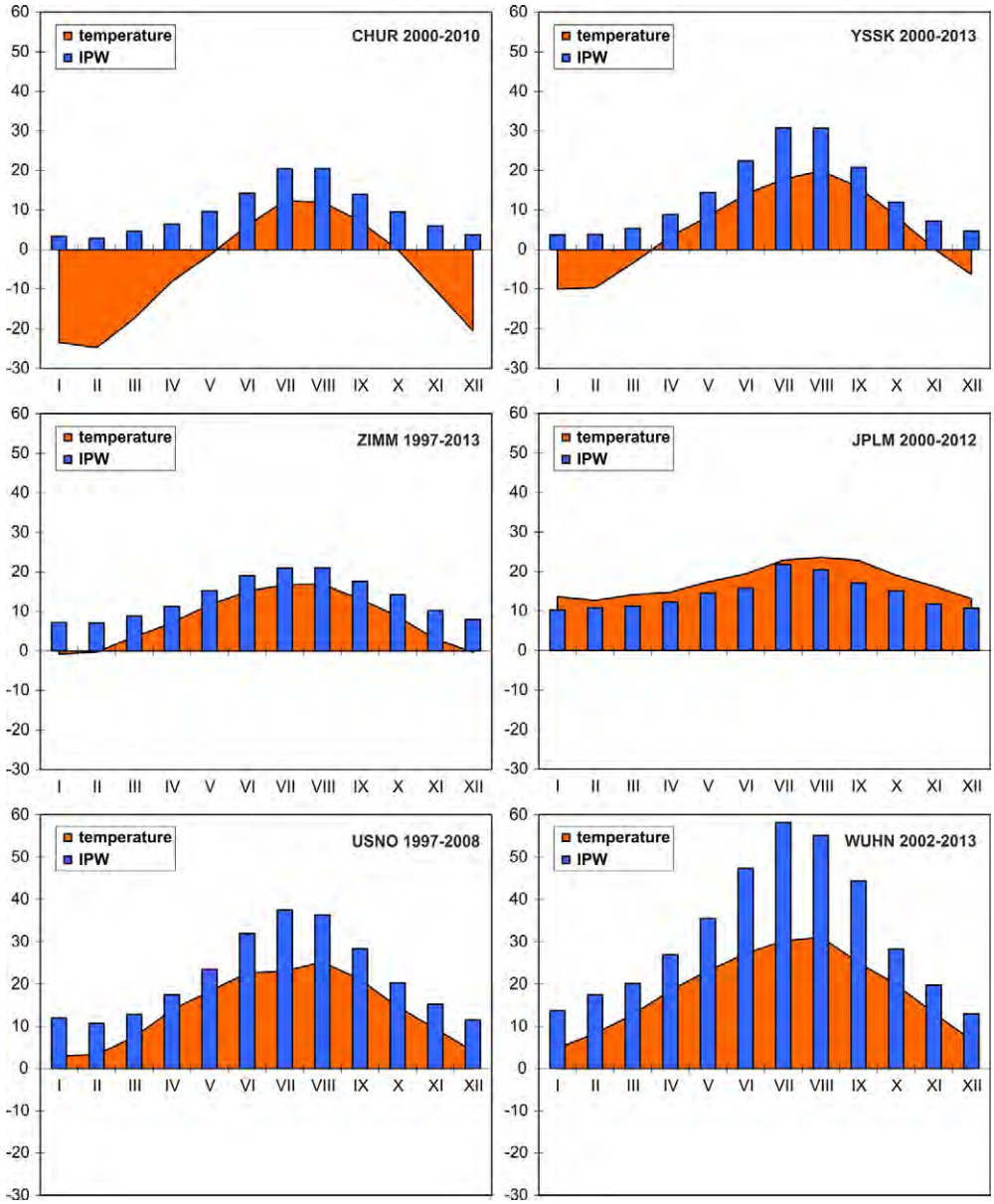

Fig. 18. Climatologic chart temperature [ºC] vs. IPW [mm] for CHUR (Churchill, Manitoba, Canada), ZIMM (Zimmerwald, Switzerland), YSSK (Yushno-Sakhalinsk, Russia), JPLM (Pasadena, California, USA), USNO (Washington DC, USA) and WUHN (Wuhan, China)

- Both PRDS (Calgary, Canada) and LHAS (Lhasa, China) have an extremely continental climate, but in the case of Lhasa the signal from the summer monsoon is perceptible in the observed IPW (IPW peak in July).

4. Conclusions

IPW is a valuable climatologic parameter. It exhibits small daily changes, which proves IPW dependence more on global circulation than local surface pro-

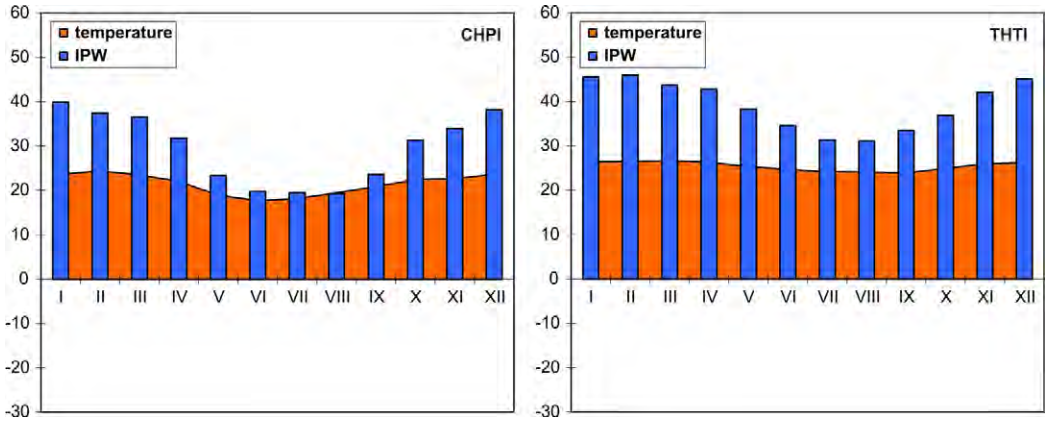

Fig. 19. Climatologic chart temperature [ºC] vs. IPW [mm] for the southern hemisphere: CHPI (Cachoeira Paulista, Sao Paulo, Brazil) and THTI (Tahiti, French Polynesia)

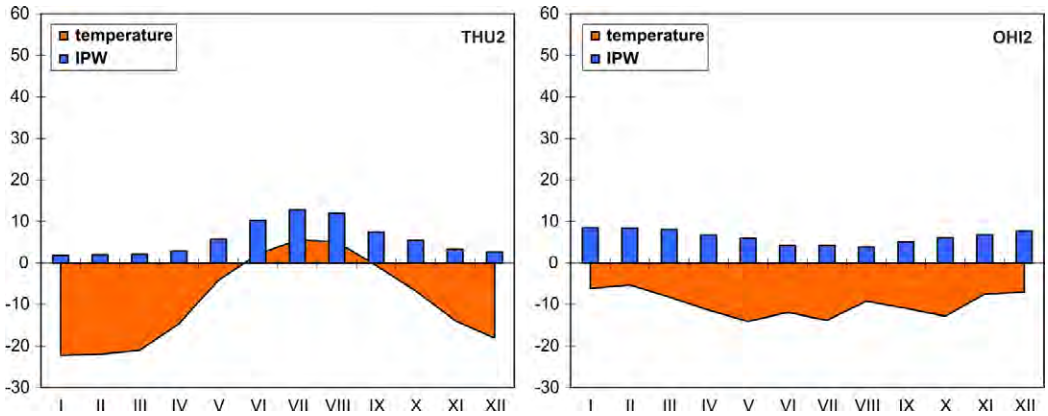

Fig. 20. Climatologic chart temperature [ºC] vs. IPW [mm] for polar stations: THU2 (Thule, Greenland) and OHI2 (Antarctica)

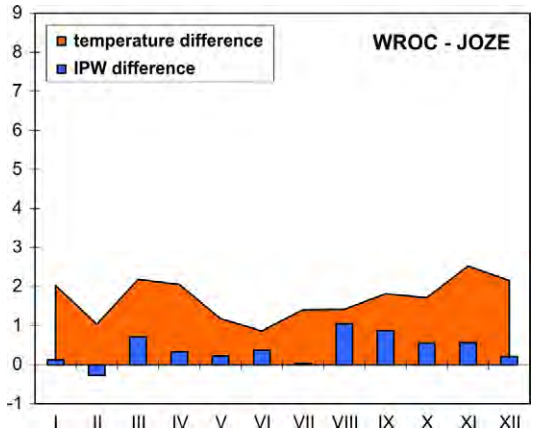

Fig. 21. Climatologic temperature [ºC] and IPW [mm] differences for relatively close stations in Poland: WROC (Wroclaw, Poland) minus JOZE (Jozefoslaw, Poland)

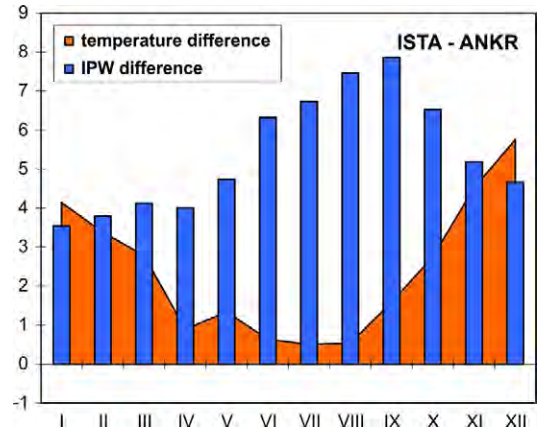

Fig. 22. Climatologic chart temperature [ºC] vs. IPW [mm] for ISTA (Istanbul, Turkey) and ANKR (Ankara, Turkey)

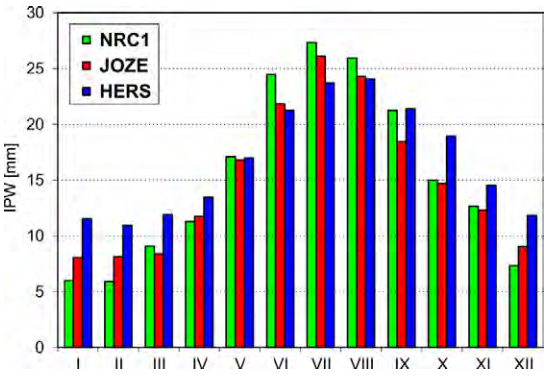

Fig. 23. IPW monthly averages for three IGS stations in the temperate climate zone of the Northern Hemisphere: NRC1 (Ottawa, Canada) is definitely continental, HERS (Hailsham, Sussex, UK) definitely oceanic, JOZE (Jozefoslaw, Poland) falls in between

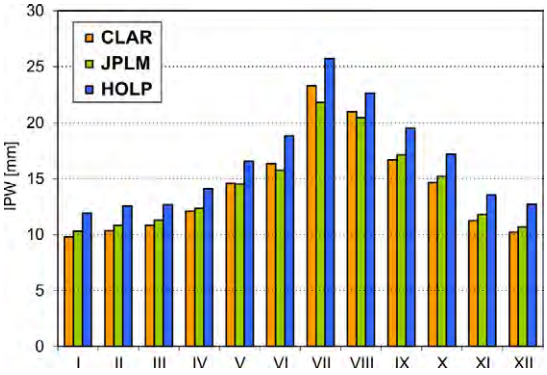

Fig. 24. IPW monthly averages for three stations in the Los Angeles area, California, USA: CLAR (Claremont), JPLM (Pasadena) and HOLP (Hollydale)

cesses (radiation, evaporation, etc.). IPW from IGS tropospheric products can be treated as an information source for aerology; it demonstrates some clear physical effects evoked by station location (e.g. elevation and changes in ZTD correlation coefficient as a function of distance) and weather patterns like dominant wind directions. Even some local climate characteristics can be distinguishable when neatly analysing monthly averages of IPW for nearby stations. IPW exhibits an evident relation with local temperature and atmospheric pressure. IPW – pressure and IPW – temperature correlation coefficients depend not only on region but also on

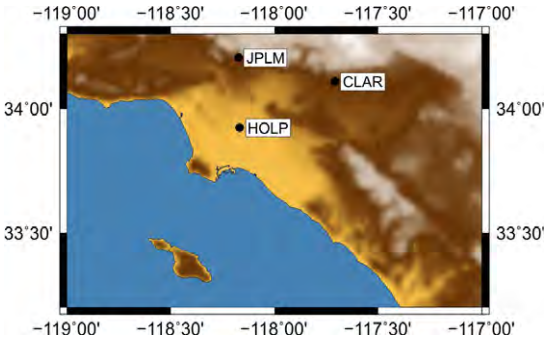

Fig. 25. IGS stations CLAR, JPLM and HOLP location map (by GMT)

season and can be explained by analysing active atmospheric air masses in the region. Charts of IPW monthly averages can serve as a variant of climate characteristic graphs.

Acknowledgements

This research was financially supported by the grant No. N N526 074038 of the Polish Ministry of Science and Higher Education / National Science Centre. The author acknowledges the work of IGS staff, especially IGS tropospheric delay product developers: Gerd Gend, Yoaz Bar-Sever, Sung Byun and Sharyl Byram as well as EPN tropospheric product providers: Wolfgang Söhne and Rosa Pacione. Radoslaw Grajczyk tested some of the ideas presented in his MSc. Thesis (2014). The map in Figure 27 has been made by Marcin Rajner. The author would like to thank Prof. Jan Krynski for his comments and suggestions indispensible for preparing the final version of the manuscript.

References

Ahrens C.D., (2011): *Meteorology Today*, Brooks/Cole.

Andrews D.G., (2010): *An Introduction to Atmospheric Physics*, Second Edition, Cambridge University Press.

Byun S.H., Bar-Sever Y.E., (2009): *A new type of troposphere zenith path delay product of the international GNSS service*, Journal of Geodesy, Vol. 83, pp. 367–373, doi: 10.1007/s00190-008-0288-8

Davis J.L., Herring T.A., Shapiro I.I., Rogers A.E., Elgered G., (1985): *Geodesy by radio interferometry: Effects of atmospheric modelling errors on estimates of baseline length*, Radio Sci., 20, pp. 1593-1607, doi:10.1029/RS020i006p01593

Duan J., Bevis M., Fang P., Bock Y., Chiswell S., Businger S., Rocken C., Solheim F., Van Hove T., Ware R., McClusky S., Herring T.A., King R.W., (1996): *GPS meteorology: direct estimation of the absolute value of precipitable water*, J. Applied Met. 35, pp. 830–838, doi:10.1175/1520-0450

Hofmann-Wellenhof B., Lichtenegger H., Wasle E., (2008): *GNSS – Global Navigation Satellite Systems GPS, GLONASS, Galileo, and more*, Springer, Wien NewYork.

Van der Marel H., (2004): *COST-716 demonstration project for the near real-time estimation of integrated water vapour from GPS,* Physics and Chemistry of the Earth, Parts A/B/C, 29, pp. 187–199.

McIlven R., (2010): *Fundamentals of Weather and Climate*, Second Edition, Oxford University Press.

Rocken C., Ware R., Van Hove T., Solheim F., Alber C., Johnson J., Bevis M., Businger S., (1993): *Sensing atmospheric water vapor with the Global Positioning System*, Geophys. Res. Lett., 20, 2631.

Salby M.L., (2012): *Physics of the Atmosphere and Climate*, Cambridge University Press.

Shelton M.L., (2009): *Hydrometeorology. Perspectives and Applications*, Cambridge University Press.

Söhne W., Weber G., (2009): *Status Report of the EPN Special Project "Troposphere Parameter Estimation"*, EUREF Publication No 15 Mitteilungen des Bundesamtes für Kartographie und Geodäsie 42(15), pp. 79–82.

Vazquez G.E., Brzezinska D., (2012): *GPS-PWV estimation and validation with radiosonde data and numerical weather prediction model in Antarctica*, GPS Solutions, doi:10.1007/s10291-012-0258-8

Kolumnowa zawartość pary wodnej (IPW) w atmosferze z pomiarów GNSS jako parametr klimatologiczny

Michał Kruczyk
Katedra Geodezji i Astronomii Geodezyjnej, Politechnika Warszawska,
Pl. Politechniki 1, 00-661, Warszawa
Tel/Fax: +48 22 2347754, E-mail: kruczyk@gik.pw.edu.pl

Streszczenie: Obliczane opóźnienia troposferyczne (czyli tak zwany produkt troposferyczny) są standardowym efektem działalności międzynarodowych służb: Międzynarodowej Służby GNSS (IGS) i Permanentnej Sieci EUREF (EPN) dostarczają cennych informacji wykorzystywanych w meteorologii i klimatologii. Długie serie rozwiązań scałkowanej (kolumnowej) zawartości pary wodnej (IPW) po odpowiednim uśrednieniu w przedziałach godzinnym, dobowym i miesięcznym mogą służyć jako indykatory lokalnego klimatu. Zmienność IPW jest zdeterminowana w pierwszym rzędzie przez cyrkulację globalną atmosfery, co potwierdzają wyniki analiz korelacji IPW z podstawowymi parametrami meteorologicznymi rejestrowanym i na stacjach GNSS. Szczególnie interesujące są zmiany współczynnika korelacji obliczanego w okresach miesięcznych. Ujawniają one charakterystyczne cechy lokalnej cyrkulacji w różnych regionach.
W pracy zaproponowano użycie pewnego rodzaju diagramu klimatologicznego (IPW/temperatura w odcinkach miesięcznych, uśrednione w okresie wieloletnim). Wybrane wykresy tego typu zostały przeanalizowane pod kątem cech klimatu. Poza mniej lub bardziej wyrazistą zmiennością sezonową średnie wartości IPW pozwalają wyodrębnić tak różne strefy klimatyczne, jak i szczególne cechy klimatu lokalnego.

Słowa kluczowe: para wodna, meteorologia GNSS, kolumnowa (scałkowana) zawartość pary wodnej, klimatologia pary wodnej